



저작자표시-비영리-변경금지 2.0 대한민국

이용자는 아래의 조건을 따르는 경우에 한하여 자유롭게

- 이 저작물을 복제, 배포, 전송, 전시, 공연 및 방송할 수 있습니다.

다음과 같은 조건을 따라야 합니다:



저작자표시. 귀하는 원저작자를 표시하여야 합니다.



비영리. 귀하는 이 저작물을 영리 목적으로 이용할 수 없습니다.



변경금지. 귀하는 이 저작물을 개작, 변형 또는 가공할 수 없습니다.

- 귀하는, 이 저작물의 재이용이나 배포의 경우, 이 저작물에 적용된 이용허락조건을 명확하게 나타내어야 합니다.
- 저작권자로부터 별도의 허가를 받으면 이러한 조건들은 적용되지 않습니다.

저작권법에 따른 이용자의 권리는 위의 내용에 의하여 영향을 받지 않습니다.

이것은 [이용허락규약\(Legal Code\)](#)을 이해하기 쉽게 요약한 것입니다.

[Disclaimer](#)

Master's Thesis of Science in Agricultural Biotechnology

**Development of Novel Hybrid Network
Solid-Emulsion Gel for Simulating
Animal Adipose Tissue**

동물 지방 조직을 모사하기 위한 새로운
하이브리드 네트워크 고체 에멀전 겔의 개발

August, 2023

**The Graduate School
Seoul National University
Department of Agricultural Biotechnology**

Minji Choi

Development of a Novel Hybrid Network Solid-Emulsion Gel for Simulating Animal Adipose Tissue

Advisor: Young Jin Choi

**Submitting a Master's Thesis of Science
in Agricultural Biotechnology**

August, 2023

**The Graduate School
Seoul National University**

Department of Agricultural Biotechnology

Minji Choi

**Confirming the master's thesis written by
Minji Choi**

August, 2023

Chair Pahn-Shick Chang (Seal)

Vice Chair Young Jin Choi (Seal)

Examiner Dong-Hyun Kang (Seal)

ABSTRACT

The plant-based meat analogue market grows due to environmental and health concerns. Therefore, a new approach to replace animal adipose tissue is needed. In this study, we developed the emulsion gel system using a hybrid gel network to simulate adipose tissue. The emulsion gel was created using plant-based material (soybean oil and soy protein isolate) and structured with a mixed gelling agent composed of agar and alginate. The hybrid emulsion gel mixed with alginate contained a dense network that trapped oil droplets. The hybrid emulsion gel showed increased hardness compared with the single-agar emulsion gel and exhibited elastic behavior, similar to pork belly fat. Cooking loss was highest for single agar emulsion gels and lowest for hybrid emulsion gels. Overall, our findings suggested that the hybrid gel network has improved the physical, rheological, and cooking properties of the emulsion gels and they have the potential to be fat replacers in meat products.

Keywords: fat analogue; emulsion gel; agar; alginate; hybrid gel network

Student Number: 2021-20272

CONTENTS

ABSTRACT.....	I
CONTENTS.....	I
LIST OF FIGURES	III
LIST OF TABLES	IV
I. INTRODUCTION	5
II. MATERIALS AND METHODS	7
2.1. Materials	7
2.2. Preparation of SPI-based emulsion.....	7
2.3. Optimization of minimum gelling concentration of agar-based emulsion gel.....	8
2.4. Preparation of hybrid gel-based emulsion	9
2.5. Confocal laser scanning microscopy	9
2.6. Cryo-field emission scanning electron microscopy	10
2.7. Color measurement	11
2.8. Rheological properties	11
2.9. Cooking properties.....	12
2.10. Texture profile analysis	12
2.11. Statistical analysis	13

III. RESULTS AND DISCUSSION	14
3.1. Optimal concentrations of emulsion gels.....	14
3.1.1. Optimal concentration of the SPI-based emulsion.....	14
3.1.2. Optimal minimum gelling concentration	17
3.2. Influence of alginate on emulsion gel properties	19
3.2.1. Color	19
3.2.2. Microstructure	21
3.2.3. Textural properties	24
3.2.4. Rheological properties	26
3.2.5. Cooking properties.....	29
CONCLUSION.....	32
REFERENCES	33
국문초록	38

LIST OF FIGURES

Figure 1. (a) The visual appearance and (b) CLSM images of SPI-based emulsions at different concentrations. (c) The droplet size distribution was used to determine the optimal concentration of the emulsifier.	16
Figure 2. Optimal concentrations for showing the solid property of agar-gelled emulsions: (a) Appearance of the inverted emulsion gels with different concentrations for determining minimum gelling concentrations. (b) Curves of length/width of emulsion gels with different agar ratios.	18
Figure 3. Confocal microscopy images (A) and cryo-SEM images (B) of agar emulsion gel (20% oil, 2% soybean protein, 2% agar) and alginate emulsion gel (20% oil, 2% soybean protein, 2% agar, 1% alginate).	23
Figure 4. Comparison of pork belly fat, agar emulsion gel (20% soybean oil, 2% SPI, and 2% agar), and alginate emulsion gel (20% soybean oil, 2% SPI, 2% agar, and 1% alginate) in terms of the change in G' and G'' (A) and $\tan \delta$ (B).....	28
Figure 5. The appearance of the emulsion gels and pork belly fat when before cooking and after cooking.....	30
Figure 6. Cooking loss (%) of pork belly fat, agar emulsion gel (20% soybean oil, 2% SPI, and 2% agar), and alginate emulsion gel (20% soybean oil, 2% SPI, 2% agar, and 1% alginate).	31

LIST OF TABLES

Table 1. Instrumental color coordinates of pork belly fat, agar emulsion gel (20% oil, 2% soybean protein, 2% agar) and alginate emulsion gel (20% oil, 2% soybean protein, 2% agar, 1% alginate).....	20
Table 2. Textural analysis profile of pork belly fat, agar emulsion gel (20% oil, 2% soybean protein, 2% agar), and alginate emulsion gel (20% oil, 2% soybean protein, 2% agar, 1% alginate).....	25

I. INTRODUCTION

The consumption of plant-based meat analogues that mimic the properties of meat products is increasing rapidly due to environmental and health concerns (He et al., 2020; Kumar et al., 2017; Sha & Xiong, 2020). In meat products, fat is an important contributor to organoleptic properties such as texture, taste, and appearance. The adipose tissue present in meat is composed of adipocytes and their surrounding connective tissue, which form a triple helix network made of collagen (Gandemer, 2002; Shoulders & Raines, 2009). Meat products have unique cooking and rheological properties due to the structural properties of adipose tissue. To accurately simulate animal fat, it is important to mimic these physical, rheological, and cooking properties.

An emulsion gel with a three-dimensional network formed by cross-linked polymers has shown the potential for mimicking animal adipose tissue (Farjami & Madadlou, 2019; Lin et al., 2020). Several approaches, such as emulsion gels made with vegetable oil, have previously been tried for making solidly structured gel systems that would mimic animal adipose tissue (Dreher et al., 2020; Ren et al., 2022). However, there are not many studies that have confirmed the physical and structural analysis and cooking characteristics of emulsion gels so far.

The mixed gel matrix and emulsion droplet structure could interact, and this could affect the mechanical properties of the emulsion gel (Lin et al., 2020). Therefore, we proposed a solid emulsion gel system based on a hybrid gel network containing agar and alginate. We investigated the proposed emulsion gel system's microstructure, appearance, rheological and textural properties, and cooking properties. In addition, the suitability of the emulsion gel system was investigated by comparing it with pork belly fat. This diligent approach to developing an emulsion gel system holds immense promise as a highly effective and convincing fat analogue for plant-based foods. By precisely mimicking the desirable attributes of animal fat, this study endeavours to elevate the sensory experience and acceptance of plant-based meat analogues, contributing to a sustainable and healthier culinary landscape.

II. MATERIALS AND METHODS

2.1. Materials

Soybean oil and soy protein isolate (SPI) were purchased from Ottogi Co. (Anyang, Korea) and Vixxol Co., Ltd. (Gunpo, Korea), respectively. Agar powder was purchased from Woori-ga Co. (Yangju, Korea). Sodium alginate and calcium chloride (dehydrate) were purchased from Ducksan (Incheon, Korea). Fresh pork belly fat (PBF) was obtained from a local meat market. Fluorescein isothiocyanate (FITC) was obtained from Sigma Aldrich (St. Louis, MO, USA). Nile red was obtained from the Tokyo Chemical Industry (Tokyo, Japan). All other chemicals for analysis were of ACS grade, and all solutions and emulsions were prepared in distilled water.

2.2. Preparation of SPI-based emulsion

To prepare the SPI-based emulsion, SPI powder (3.75% w/w) was dispersed in distilled water and stirred overnight for dissolution. Sodium azide (0.02% w/w) was added to inhibit the growth of microorganisms. The SPI solution was appropriately diluted to obtain the required concentration. Emulsions with various SPI concentrations (0.25%, 0.5%, 1%, 2%, and 3%

w/w) with a constant concentration of oil content (20% w/w) were prepared. The SPI –based emulsion was blended using a high-speed blender (Ultra-Turrax T25D, IKA Werke GmbH & Co., Staufen, Germany) at 12,000 rpm for 2 min. The droplet size distribution of the emulsions was measured using a light diffraction particle size analyzer (Mastersizer 3000, Malvern Instruments, Malvern, Worcestershire, United Kingdom). Samples were diluted in recirculating distilled water (2,500 rpm) during measurement. The refractive and absorption indexes were set to 1.520 and 0.100, respectively. The visual observation of the SPI–based emulsion was analyzed using digital photography.

2.3. Optimization of minimum gelling concentration of agar-based emulsion gel

Emulsion gels were prepared by varying the agar concentration (0.25%, 0.5%, 1%, 2%, and 3% w/w) to determine the minimum gelation concentration at which the emulsion was solidified. Agar powder 5% (w/w) was dispersed in distilled water and stirred overnight to ensure dissolution. The agar solutions, SPI solution, and soybean oil were allowed to reach 90°C using a water bath with constant stirring. The solutions were weighed for each concentration in a 100-ml beaker and then blended using the high-speed

blender Ultra-Turrax T25D at 12,000 rpm for 2 min. The resulting sample was cooled at room temperature for 1 h. The minimum gelation concentration was determined by observing the height/width ratio and the nonflowing behavior under the gravity of the prepared gel sample.

2.4. Preparation of hybrid gel-based emulsion

Alginate solutions were prepared at a constant concentration of 5% (w/w) and stirred overnight to ensure dissolution. Hybrid emulsion gels containing of SPI (2% w/w) and agar (2% w/w) and alginate (1% w/w) were prepared. In addition, an agar-based emulsion gel without alginate was prepared as a control sample. They were denoted as AAEG, and AEG, respectively. All solutions were allowed to reach 90°C using a water bath with constant stirring and then blended using the Ultra-Turrax T25D high-speed blender at 12,000 rpm for 2 min. The resulting sample was cooled at room temperature for 1 h. The emulsion gel containing alginate was stirred in 1% (w/w) calcium chloride solution and equilibrated for at least 30 min to complete cross-linking.

2.5. Confocal laser scanning microscopy

The microstructure of the emulsions and emulsion gels was imaged

using a confocal laser scanning microscope (SP8 X Confocal Microscope, Leica Microsystems, Mannheim, Germany) with fluorescein sodium salt (FITC) and Nile red as fluorescence dyes for the protein and oil phases, respectively. The excitation/emission wavelength of Nile red was 550/600 to 670 nm, while the excitation/emission wavelength of FITC was 488/500 to 561 nm. Both stock dye solutions (1% w/w) were mixed with the emulsions up to concentrations of approximately 0.1% (w/w). The protein phases stained with FITC appeared green, while the oil phases stained with Nile red appeared red.

2.6. Cryo-field emission scanning electron microscopy

The microstructure of the emulsion gels was examined using cryo-field emission scanning electron microscopy (Cryo-FESEM, Crossbeam 550, Carl Zeiss, Oberkochen, Germany). The emulsion gel samples were attached to an aluminum sample holder and immersed in a liquid nitrogen slush at -210°C . Then, the frozen samples were transferred to a cryo-preparation chamber and disrupted at -140°C . The fractured samples were etched at -90°C for 5 min. The sample was then coated with platinum (10 mA and 60 s) and observed at a magnification of $80.00 \text{ K} \times$ at an accelerating voltage of 10 kV.

2.7. Color measurement

The color characteristics of the sample were analyzed using a colorimeter (CR-400, Konica Minolta Sensing, Inc., Tokyo, Japan) based on the L*, a*, and b* color scale. L* denotes brightness, while a* and b* indicate red-green and yellow-blue chromaticity, respectively. The colorimeter was calibrated using a standard white plate (L*=77.38, a*=−3.47, b*=17.15) before use. The total color difference (ΔE) was calculated as follows:

$$\Delta E = \sqrt{(L_{control}^* - L_{treatment}^*)^2 + (a_{control}^* - a_{treatment}^*)^2 + (b_{control}^* - b_{treatment}^*)^2}$$

2.8. Rheological properties

The rheological properties of each sample were determined using a rheometer (RheoStress 1, Thermo Scientific™ HAAKE, Karlsruhe, Germany). The samples (2 g) were loaded between a parallel plate geometry of 20 mm in diameter. The gap between the Peltier plate and the geometry plate was set at 1 mm, silicone oil was applied, and a solvent trap module was used to prevent moisture loss during the test. Samples were conditioned on a Peltier plate for 10 min at the initial measurement temperature. Then, a frequency sweep test was performed at 0.1 to 10 Hz and 0.1% strain (in the linear viscoelastic range) at 25°C.

2.9. Cooking properties

The cooking properties of the emulsion gels were compared with those of meat fat using appearance after cooking and cooking loss. The emulsion gel and meat fat were cooked in boiling to 100 °C for 8min and 40min, respectively, based on an internal temperature of 70°C. After cooking, images were acquired by operating a camera fixed inside a photo box with a light source. Cooking loss was determined after cooking and cooling to 25 °C. Cooking loss was calculated as follows:

$$\text{Cooking loss (\%)} = \frac{W_b - W_a}{W_b} \times 100$$

where W_b is weight before cooking (g), W_a is weight after cooking (g)

2.10. Texture profile analysis

The texture profile analysis (TPA) of the emulsion gel and pork belly fat was measured using a texture analyzer (TA.XT plus, Stable Micro Systems, Godalming, Surrey, UK). The sample was cut into cubes (1 × 1 × 1 cm) and conditioned at 25°C. The TPA testing was performed using a P/100 probe (100 mm diameter) at 40% strain and a crosshead speed of 2 mm/s.

2.11. Statistical analysis

Each experiment was repeated three times for each condition. The one-way analysis of variance (ANOVA) was used to analyze the data, which were presented as the mean plus or minus the standard deviation (SD). In addition, Tukey's HSD multiple-range test examined significant differences at a p -value of less than 0.05. All statistical calculations and analyses were performed using SPSS software (version 25.0, SPSS, Inc., Chicago, IL, USA).

III. RESULTS AND DISCUSSION

3.1. Optimal concentrations of emulsion gels

3.1.1. Optimal concentration of the SPI-based emulsion

Soy protein isolate is commonly used as an emulsifier in food systems to stabilize oil droplets and reduce their size (Lin et al., 2021). We optimized the concentration of SPI to achieve sufficient emulsification of the soybean oil, based on the emulsion's appearance, microstructure, and droplet size distribution analysis. Fig. 1a shows the appearance of emulsions containing different concentrations of SPI from 0% to 3%. Emulsions with 0.25%, 0.5%, and 1% SPI solutions exhibited rapid phase separation between the oil and water phases, indicating that the emulsifier concentration was insufficient to cover the oil droplets (McClements & Jafari, 2018). In contrast, emulsions containing more than 2% SPI showed a stable dispersion. The microstructure was analyzed using CLSM (see Fig. 1b). The red-dyed oil droplets were uniformly distributed in the green-dyed protein solution, and the number of oil droplets increased while their size decreased with an increasing SPI concentration. Droplet size distribution is one of the essential indicators that can confirm the stability of the emulsion (Nour, 2018). As the SPI

concentration increased from 0.25% to 0.5%, the droplet size shifted toward a smaller distribution (see Fig. 1c). These results suggested that an amount of SPI of more than 2% is required to form stable SPI-based emulsions.

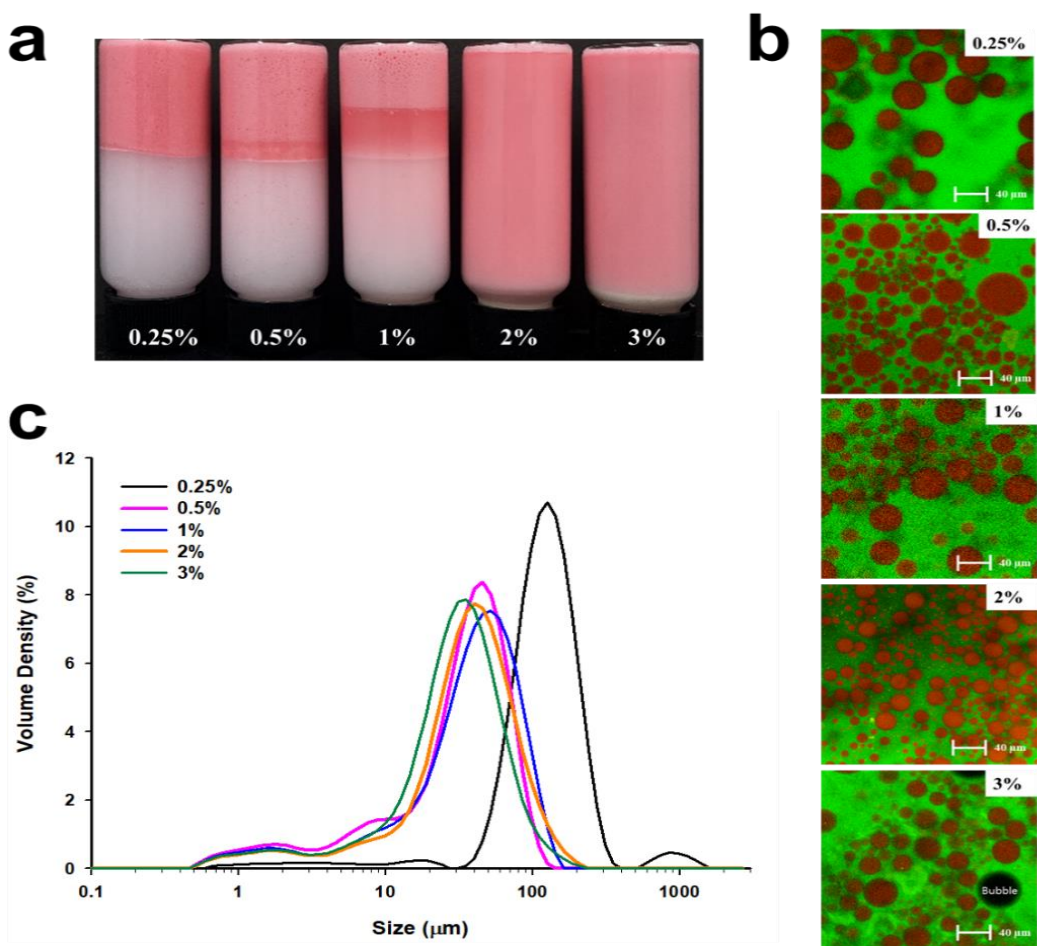


Figure 1. (a) The visual appearance and (b) CLSM images of SPI-based emulsions at different concentrations. (c) The droplet size distribution used to determine the optimal concentration of emulsifier.

3.1.2. Optimal minimum gelling concentration

Emulsion gels prepared using an appropriate gelation process can improve the sensory and physical properties of processed foods (Ren et al., 2022). Specifically, to achieve the textural characteristics of adipose tissue, the matrix gel molecular concentration must be higher than the critical gelation concentration (Lin et al., 2020). Emulsion gels with different agar concentrations were prepared to determine the critical gelation concentration at which the emulsion solidified. Visual observation of the samples indicated that a gel with a rigid structure was formed when the agar concentration was 2% or higher (Fig. 2a). Agar is known to form gels by generating hydrogen bonds between polysaccharide molecules (Tako et al., 2021). The height/width ratio of the emulsion gel was observed to confirm that the gel maintained its shape against gravity (see Fig. 2b). At low agar concentrations, the height/width ratio was low, indicating that the gel strength was weaker than gravity and could not maintain the structure. When the agar concentration exceeded 2%, the height/width ratio remained consistent, suggesting a stable gel. Therefore, the appropriate agar ratio for gelling the emulsion was fixed at 2%.

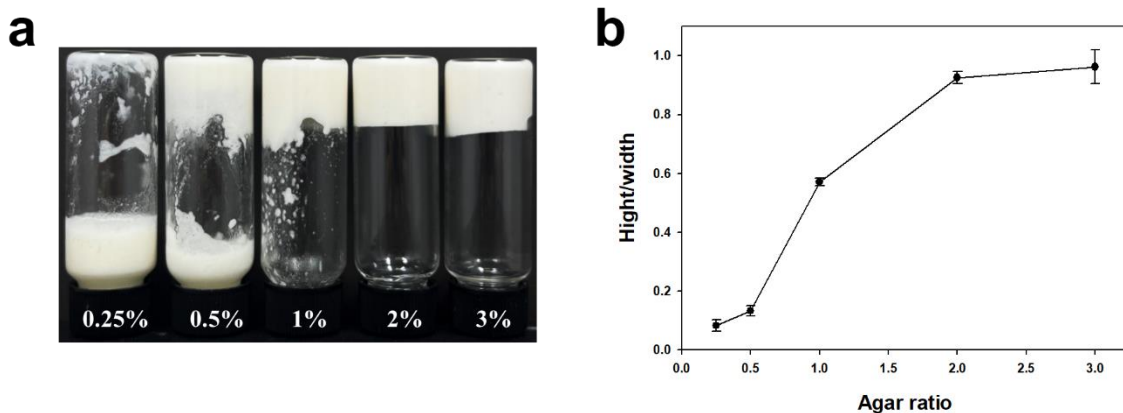


Figure 2. Optimal concentrations for showing the solid property of agar-gelled emulsions: (a) Appearance of the inverted emulsion gels with different concentrations for determining minimum gelling concentrations. (b) Curves of length/width of emulsion gels with different agar ratios.

3.2. Influence of alginate on emulsion gel properties

3.2.1. Color

Color is a crucial factor in meat and meat analogues as it affects consumer preferences (Bohrer, 2019). Table 1 shows the colors of pork belly fat and emulsion gels. The emulsion gels had a higher L^* value than the pork belly fat because the oil droplets in the emulsion gel were smaller than the adipocytes in adipose tissue, leading to more significant light scattering (Hu & McClements, 2022). Emulsion gels had a slightly green color compared with the red color of adipose tissue. However, the values of a^* for all of the emulsion gels ranged from -0.2 to 0.1 , indicating that they exhibited little red-green hue. The emulsion gel made of soybean oil and SPI showed a higher yellow color than pork belly fat due to the presence of chromophores such as carotenoids in soybeans (Scholfield & Dutton, 1954). There was no significant difference in the ΔE of the emulsion gels, indicating that the alginate concentration had little effect on the color of the emulsion gels.

Table 1. Instrumental color coordinates of pork belly fat, agar emulsion gel (20% oil, 2% soybean protein, 2% agar) and alginate emulsion gel (20% oil, 2% soybean protein, 2% agar, 1% alginate).

Sample	L*	a*	b*	ΔE
Pork belly fat	81.01±0.37 ^a	4.82±0.65 ^b	5.59±0.19 ^a	
AEG	97.20±0.21 ^b	−0.42±0.01 ^a	8.21±0.10 ^c	17.22±0.27 ^a
AAEG	98.14±0.14 ^{bc}	−0.19±0.01 ^a	7.46±0.04 ^b	17.64±0.41 ^a

3.2.2. Microstructure

The microstructure of the emulsion gels was analyzed using CLSM and cryo-SEM. Fig. 3 shows microstructural images of emulsion gels. The CLSM images indicated that the size of the oil droplets decreased with a containing alginate. Increasing polymer content increased the viscosity of the aqueous phase, leading to higher shear forces during mixing, which can result in smaller droplet formation (Lee et al., 1957). These results were consistent with those of previous research demonstrating that higher shear forces generated during blending can result in the formation of smaller droplets (Hu & McClements, 2022). Furthermore, the SEM images showed that the emulsion gels had significantly different microstructures. The pore size of the emulsion gel containing alginate was smaller than that of the agar emulsion gel. These structural changes may be due to intermolecular hydrogen bonds and interactions of the gel network (Donohue, 1952). Agar and alginate contain large numbers of hydroxyl groups that can form hydrogen bonds and induce interactions (Zeng et al., 2015). In this system, the hybrid emulsion gel had a dense network structure because of the interactions of the hydrogen bonds formed between the agar and alginate and the formation of gel structures of different sizes. In the case of agar gel, seven to 11 double helices were assembled into a bundle to form a gel network with various pore sizes from

100 to 1200 nm. Additionally, alginate formed a rod-shaped cross-linked complex with divalent cations and had tiny pores of 5 to 7 nm in length (Chau et al., 2015).

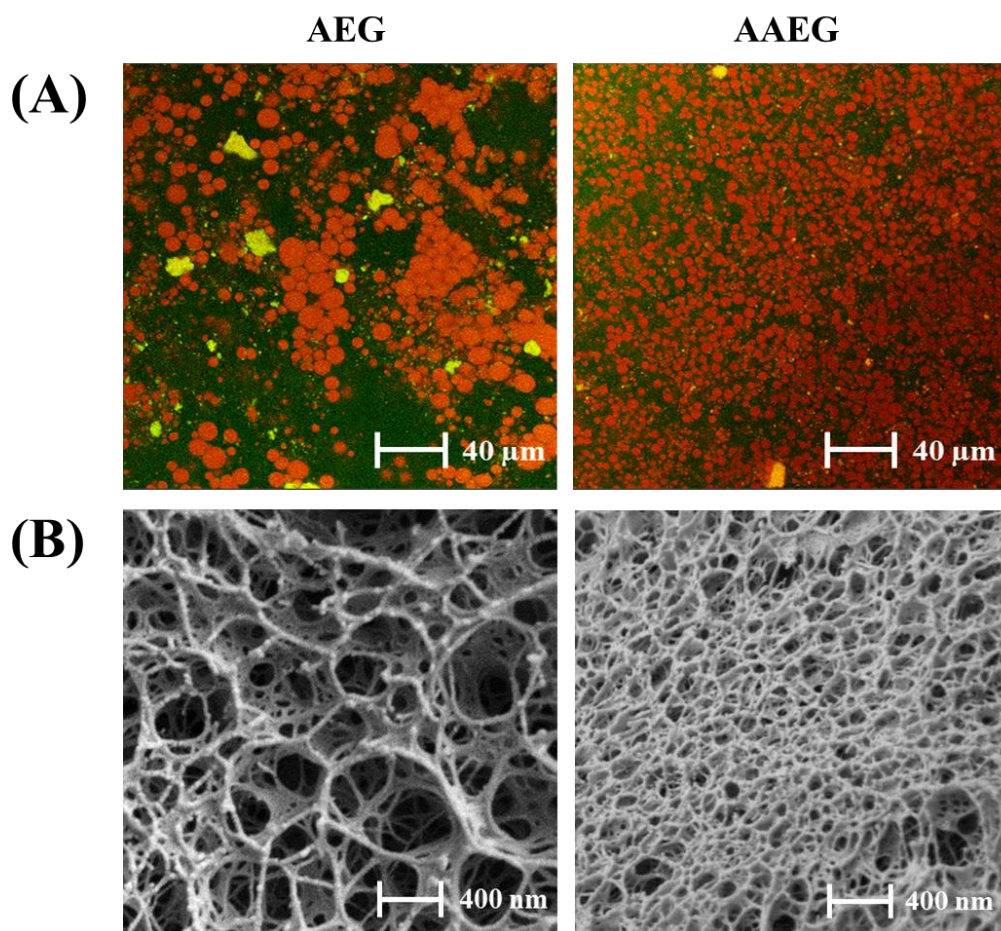


Figure 3. Confocal microscopy images (A) and cryo-SEM images (B) of agar emulsion gel (20% oil, 2% soybean protein, 2% agar) and alginate emulsion gel (20% oil, 2% soybean protein, 2% agar, 1% alginate).

3.2.3. Textural properties

The textures of the fat and oil contribute to the tenderness and mouthfeel of plant-based meat products (Bohrer, 2019). Table 2 presents the textural properties of pork belly fat and the emulsion gels, including their hardness, adhesiveness, springiness, cohesiveness, and chewiness. In the emulsion gel containing alginate, the hardness and chewiness increased, indicating the formation of a dense gel structure due to the increase in intermolecular bonds and interactions (Huang, Xiao, Zhou, Li, Liu, & Zeng, 2020; Huang et al., 2020; Seman, 2008). Emulsion gel containing alginate has increased hardness and chewiness compared to emulsion gels without alginate. Therefore, a dense gel structure with increased intermolecular bonds and interactions can improve the physical properties of emulsion gels, which showed the potential to mimic animal adipose tissue in food processing.

Table 2. Textural analysis profile of pork belly fat, agar emulsion gel (20% oil, 2% soybean protein, 2% agar), and alginate emulsion gel (20% oil, 2% soybean protein, 2% agar, 1% alginate).

Sample type	Hardness (N)	Adhesiveness (N.s)	Springiness	Cohesiveness	Chewiness
PBF	11.08±0.63 ^c	-4.47±1.93 ^{ab}	0.78±0.04 ^a	0.54±0.05 ^b	480.82±95.80 ^b
AEG	2.75±0.04 ^a	-8.48±3.86 ^a	1.11±0.07 ^b	0.19±0.01 ^a	59.91±8.60 ^a
AAEG	9.83±0.45 ^b	-2.22±1.40 ^b	0.67±0.04 ^a	0.20±0.01 ^a	136.04±22.97 ^a

3.2.4. Rheological properties

The rheological properties of plant-based adipose tissue affect the texture and sensory properties of meat analogues (McClements et al., 2021). Therefore, frequency sweep tests were investigated within the limits of the viscoelastic range to determine the frequency dependence of storage moduli (G'), loss moduli (G''), and $\tan \delta$ of the pork belly fat and emulsion gels (Fig. 4). As shown in Fig 4A, all samples showed a higher G' value than G'' in the entire frequency range, showing that they behave like elastic solids or gels. The pork belly fat exhibited a higher storage modulus than all the emulsion gels due to the high elastic properties of the collagen component (Lepetit, 2008). The AA emulsion gel showed a higher modulus value than the A emulsion, indicating that the double network contributed to improving the elastic properties of the emulsion gel. These results are consistent with those obtained in texture profile analysis, suggesting that the interaction between the mixed gel matrix can enhance the rheological properties of the gel (dos Santos Araújo et al., 2019).

The dynamic viscoelastic behavior of the samples was clearly shown using $\tan \delta$, which is a function of G''/G' . All samples exhibit $\tan \delta$ values less than 1 and have solid or gel-like properties. (see Fig. 4B). The $\tan \delta$ of pork belly fat reached a maximum of 0.5 and then decreased to 0.29. The reduction in $\tan \delta$

in pork belly fat is likely a result of the plastic properties of the fat crystal network inside the adipocytes (Wijarnprecha, Gregson, Sillick, Fuhrmann, Sonwai, & Rousseau, 2022). The emulsion gel showed little dependence on the irradiated frequency, with a value of about 0.1, indicating a highly elastic and solid-like gel behavior. These results suggested that the hybrid gel network including alginate could improve the gel strength and rheological properties of emulsion gels, making them potential for simulating animal fat.

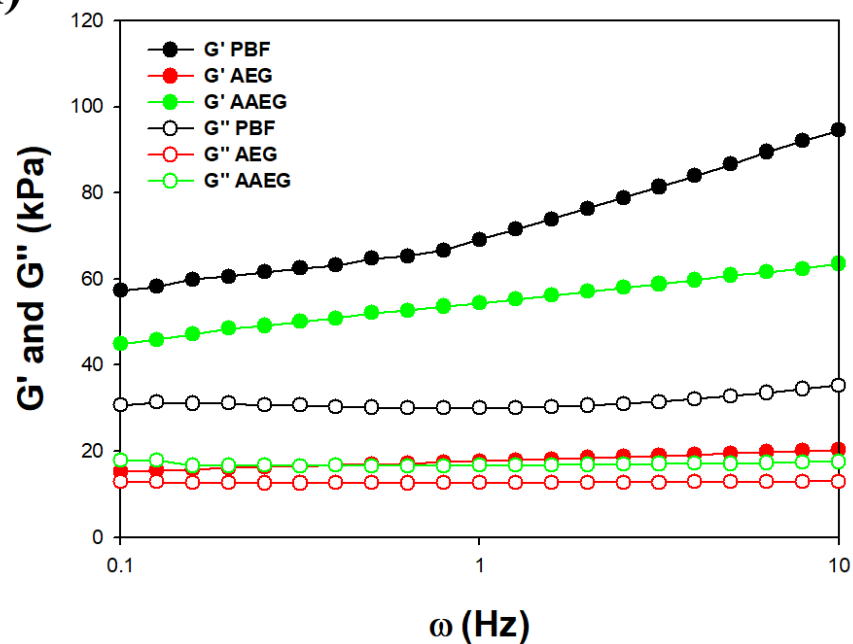
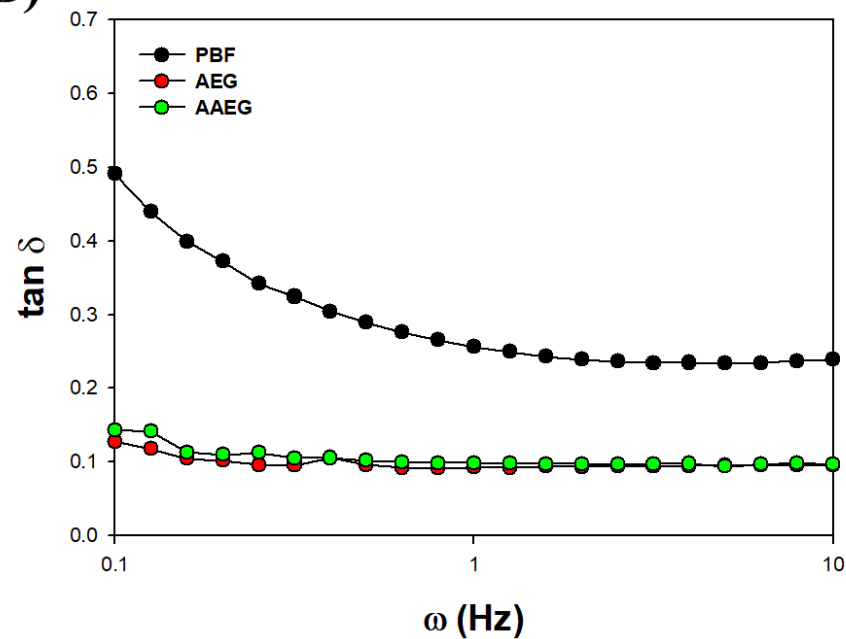
(A)**(B)**

Figure 4. Comparison of pork belly fat, agar emulsion gel (20% soybean oil, 2% SPI, and 2% agar), and alginate emulsion gel (20% soybean oil, 2% SPI, 2% agar, and 1% alginate) in terms of the change in G' and G'' (A) and $\tan \delta$ (B).

3.2.5. Cooking properties

To evaluate the cooking properties of the samples, the appearance after cooking and the amount of loss during cooking were measured. Cooking properties acts as an important factor related to food quality and product yield when consumed. Figure 5 shows the appearance of pork belly fat and emulsion gel before and after cooking. In the case of AEG, the structure collapsed due to melting of the agar structure and the gel shape could not be maintained. However, the AAEG maintained its gel shape. This indicates that the denser gel structure with an increase in molecular interactions in the hybrid gel network has stability even at cooking temperature.

As shown in Fig. 6, AEG was completely water soluble, while AAEG showed a low cooking loss of about 2%. These results can be attributed to the reduced loss during cooking as the dense gel structure of agar and alginate strongly traps the emulsion oil droplets in the network. In general, high cooking loss after cooking may be related to the organoleptic properties of foods and therefore low consumer palatability, so densely structured emulsion gels have the potential to be good quality fat substitutes.

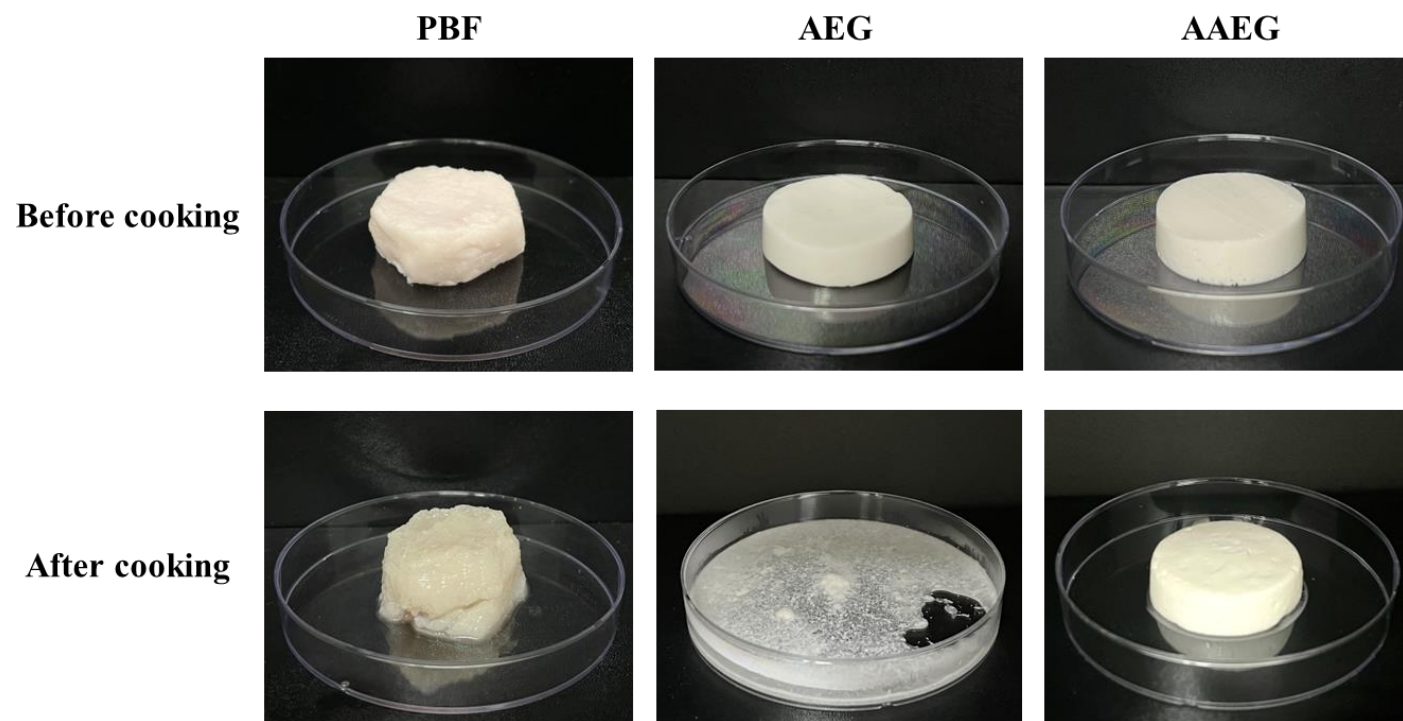


Figure 5. Appearance of the emulsion gels and pork belly fat when before cooking and after cooking.

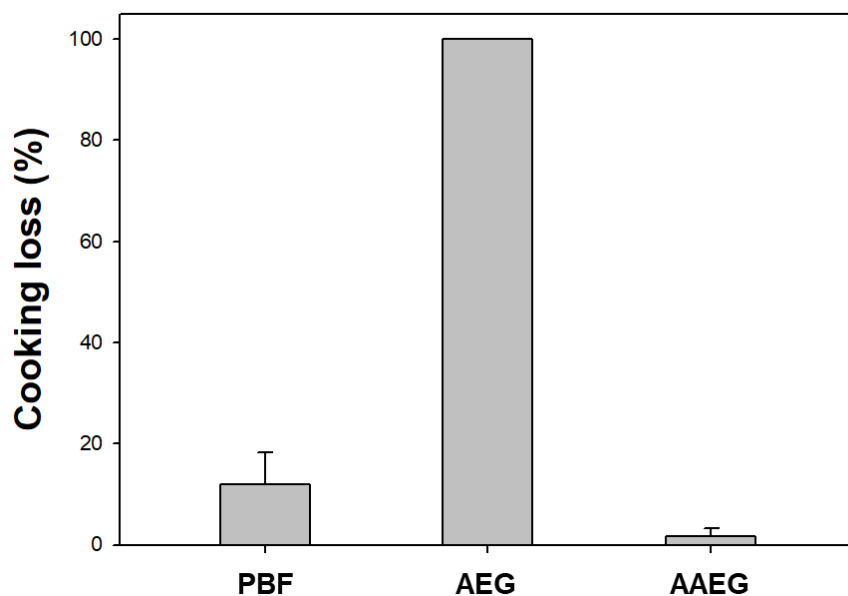


Figure 6. Cooking loss (%) of pork belly fat, agar emulsion gel (20% soybean oil, 2% SPI, and 2% agar), and alginate emulsion gel (20% soybean oil, 2% SPI, 2% agar, and 1% alginate).

CONCLUSION

In this study, a solid emulsion gel system was developed using a hybrid gel network composed of agar and alginate to simulate animal adipose tissue. The properties of the emulsion gels were significantly influenced by the gel network. Emulsion gels containing only agar had weak hardness and high cooking loss due to their sparse gel structure. In contrast, the hybrid emulsion gels exhibited denser gel structures, leading to improved hardness and low cooking loss. Rheological analysis indicated that the formed hybrid gel network enhanced the strength of emulsion gel and exhibit elastic properties. These results demonstrated that the physical and cooking properties of the emulsion gels were significantly improved due to the intermolecular bonding and interactions of the gel network. The hybrid emulsion gel system successfully simulated the desirable properties of pork belly fat, and this indicated that the system has the potential to be an adipose tissue substitute in plant-based meat analogue products.

REFERENCES

- Amaya-Gonzalez, S., de-Los-Santos-Álvarez, N., Miranda-Ordieres, A. J., & Lobo-Castanon, M. J. (2014). Aptamer binding to celiac disease-triggering hydrophobic proteins: a sensitive gluten detection approach. *Analytical chemistry*, 86(5), 2733-2739.
- Biesiekierski, J. R. (2017). What is gluten? *Journal of gastroenterology and hepatology*, 32, 78-81.
- Bottari, F., Moretto, L. M., & Ugo, P. (2018). Impedimetric sensing of the immuno-enzymatic reaction of gliadin with a collagen-modified electrode. *Electrochemistry Communications*, 97, 51-55.
- Chang, C.-C., Chen, C.-Y., Zhao, X., Wu, T.-H., Wei, S.-C., & Lin, C.-W. (2014). Label-free colorimetric aptasensor for IgE using DNA pseudoknot probe. *Analyst*, 139(13), 3347-3351.
- Chiriaco, M. S., de Feo, F., Primiceri, E., Monteduro, A. G., de Benedetto, G. E., Pennetta, A., . . . Maruccio, G. (2015). Portable gliadin-immunochip for contamination control on the food production chain. *Talanta*, 142, 57-63.
- CODEX, S. (2008). STAN 118-1979. Standard for foods for special dietary use for persons intolerant to gluten.

- Commission, E. (2014). Commission implementing regulation (EU) No 828/2014 of 30 July 2014 on the requirements for the provision of information to consumers on the absence or reduced presence of gluten in food. Off J Eur Union, 228, 5-8.
- Darmostuk, M., Rimpelova, S., Gbelcova, H., & Ruml, T. (2015). Current approaches in SELEX: An update to aptamer selection technology. *Biotechnology advances*, 33(6), 1141-1161.
- Diaz-Amigo, C., & Popping, B. (2013). Accuracy of ELISA detection methods for gluten and reference materials: a realistic assessment. *Journal of agricultural and food chemistry*, 61(24), 5681-5688.
- Epanchintseva, A., Vorobjev, P., Pyshnyi, D., & Pyshnaya, I. (2018). Fast and strong adsorption of native oligonucleotides on citrate-coated gold nanoparticles. *Langmuir*, 34(1), 164-172.
- Gomaa, A., & Boye, J. (2015). Simultaneous detection of multi-allergens in an incurred food matrix using ELISA, multiplex flow cytometry and liquid chromatography mass spectrometry (LC–MS). *Food Chemistry*, 175, 585-592.
- Gopinath, S. C., Lakshmipriya, T., & Awazu, K. (2014). Colorimetric detection of controlled assembly and disassembly of aptamers on unmodified gold nanoparticles. *Biosensors and Bioelectronics*, 51,

115-123.

Guo, Y., Zhang, Y., Shao, H., Wang, Z., Wang, X., & Jiang, X. (2014). Label-free colorimetric detection of cadmium ions in rice samples using gold nanoparticles. *Analytical chemistry*, 86(17), 8530-8534.

Holzhauser, T., Johnson, P., Hindley, J. P., O'Connor, G., Chan, C.-H., Costa, J., . . . Miani, M. (2020). Are current analytical methods suitable to verify VITAL® 2.0/3.0 allergen reference doses for EU allergens in foods? *Food and Chemical Toxicology*, 145, 111709.

Khansili, N., Rattu, G., & Krishna, P. M. (2018). Label-free optical biosensors for food and biological sensor applications. *Sensors and Actuators B: Chemical*, 265, 35-49.

Loveday, S. M. (2020). Plant protein ingredients with food functionality potential. *Nutrition Bulletin*, 45(3), 321-327.

Malvano, F., Albanese, D., Pilloton, R., & Di Matteo, M. (2017). A new label-free impedimetric aptasensor for gluten detection. *Food Control*, 79, 200-206.

Mujico, J. R., Lombardía, M., Mena, M. C., Méndez, E., & Albar, J. P. (2011). A highly sensitive real-time PCR system for quantification of wheat contamination in gluten-free food for celiac patients. *Food Chemistry*, 128(3), 795-801.

- Pinto, A., Polo, P. N., Henry, O., Redondo, M., Svobodova, M., & O'Sullivan, C. K. (2014). Label-free detection of gliadin food allergen mediated by real-time apta-PCR. *Analytical and bioanalytical chemistry*, 406(2), 515-524.
- Ramalingam, S., Elsayed, A., & Singh, A. (2020). An electrochemical microfluidic biochip for the detection of gliadin using MoS₂/graphene/gold nanocomposite. *Microchimica Acta*, 187(12), 1-11.
- Scharf, A., Kasel, U., Wichmann, G., & Besler, M. (2013). Performance of ELISA and PCR methods for the determination of allergens in food: an evaluation of six years of proficiency testing for soy (*Glycine max* L.) and wheat gluten (*Triticum aestivum* L.). *Journal of agricultural and food chemistry*, 61(43), 10261-10272.
- Scherf, K. A., & Poms, R. E. (2016). Recent developments in analytical methods for tracing gluten. *Journal of Cereal Science*, 67, 112-122.
- Scherf, K. A., Wieser, H., & Koehler, P. (2016). Improved quantitation of gluten in wheat starch for celiac disease patients by gel-permeation high-performance liquid chromatography with fluorescence detection (GP-HPLC-FLD). *Journal of agricultural and food chemistry*, 64(40), 7622-7631.

- Svigelj, R., Dossi, N., Grazioli, C., & Toniolo, R. (2022). based aptamer-antibody biosensor for gluten detection in a deep eutectic solvent (DES). *Analytical and bioanalytical chemistry*, 414(11), 3341-3348.
- Tanner, G. J., Colgrave, M. L., Blundell, M. J., Goswami, H. P., & Howitt, C. A. (2013). Measuring hordein (gluten) in beer—a comparison of ELISA and mass spectrometry. *PLoS One*, 8(2), e56452.
- Wu, Y.-Y., Huang, P., & Wu, F.-Y. (2020). A label-free colorimetric aptasensor based on controllable aggregation of AuNPs for the detection of multiplex antibiotics. *Food Chemistry*, 304, 125377.
- Zhang, W., Wang, Y., Nan, M., Li, Y., Yun, J., Wang, Y., & Bi, Y. (2021). Novel colorimetric aptasensor based on unmodified gold nanoparticle and ssDNA for rapid and sensitive detection of T-2 toxin. *Food Chemistry*, 348, 129128.

국문초록

식물성 육류 유사품 시장은 환경 및 건강 문제로 인해 성장하고 있습니다. 따라서 동물의 지방조직을 대체하기 위한 새로운 접근이 필요합니다. 본 연구에서는 지방 조직을 시뮬레이션하기 위해 하이브리드 겔 네트워크를 사용하여 에멀전 겔 시스템을 개발했습니다. 에멀전 겔은 식물 기반 물질(대두유 및 콩 단백질 분리물)을 사용하여 만들어졌으며 한천과 알지네이트로 구성된 혼합 겔 화제로 구성되었습니다. 알지네이트와 혼합된 하이브리드 에멀전 겔은 기름 방울을 가두는 조밀한 네트워크를 포함했습니다. 요리 손실은 단일 한천 에멀전 겔에서 가장 높았고 하이브리드 에멀전 겔에서 가장 낮았습니다. 하이브리드 에멀전 겔은 단일 한천 에멀전 겔에 비해 경도가 증가하였고 돼지 지방 조직과 유사한 탄성 거동을 보였습니다. 전반적으로, 본 연구 결과는 하이브리드 겔 네트워크가 에멀전 겔의 물리적, 유변학적 및 요리 특성을 개선했으며 육류 제품에서 지방을 대체할 가능성이 있음을 시사합니다.

주요어: 지방 유사체; 에멀전 겔; 한천; 알기네이트; 하이브리드 겔 네트워크

학번: 2021-20272